

The *Arabidopsis* *JAGGED* gene encodes a zinc finger protein that promotes leaf tissue development

Carolyn K. Ohno, G. Venugopala Reddy, Marcus G. B. Heisler and Elliot M. Meyerowitz*

Division of Biology 156-29, California Institute of Technology, 1200 East California Boulevard, Pasadena, CA 91125, USA

*Author for correspondence (e-mail: meyerow@its.caltech.edu)

Accepted 18 November 2003

Development 131, 1111-1122
Published by The Company of Biologists 2004
doi:10.1242/dev.00991

Summary

Important goals in understanding leaf development are to identify genes involved in pattern specification, and also genes that translate this information into cell types and tissue structure. Loss-of-function mutations at the *JAGGED* (*JAG*) locus result in *Arabidopsis* plants with abnormally shaped lateral organs including serrated leaves, narrow floral organs, and petals that contain fewer but more elongate cells. *jag* mutations also suppress bract formation in *leafy*, *apetala1* and *apetala2* mutant backgrounds. The *JAG* gene was identified by map-based cloning to be a member of the zinc finger family of plant transcription factors and encodes a protein similar in

structure to SUPERMAN with a single C₂H₂-type zinc finger, a proline-rich motif and a short leucine-rich repressor motif. *JAG* mRNA is localized to lateral organ primordia throughout the plant but is not found in the shoot apical meristem. Misexpression of *JAG* results in leaf fusion and the development of ectopic leaf-like outgrowth from both vegetative and floral tissues. Thus, *JAG* is necessary for proper lateral organ shape and is sufficient to induce the proliferation of lateral organ tissue.

Key words: *JAGGED*, Lateral organ growth, Leaf morphogenesis, Leaf development, *Arabidopsis thaliana*

Introduction

Lateral organs (leaves and floral organs) develop as outgrowths from the flanks of the shoot apical meristem (SAM). During their growth, cell division and differentiation must be coordinated along three principal axes: a proximal-distal axis, along which the proximal petiole and the distal blade are positioned; an adaxial-abaxial axis defining the position of tissues that abut the meristem versus those located farther away; and a medial-lateral axis that defines the position of the central midrib relative to the lateral blade and leaf margins. Recent studies have uncovered a large number of genes that specify adaxial/abaxial patterning including *PHANTASTICA* (*PHAN*) (Waites and Hudson, 1995; Waites et al., 1998), *PHABULOSA* and *PHAVOLUTA* (*PHB* and *PHV*) (McConnell and Barton, 1998; McConnell et al., 2001), *ARGONAUTE* (*AGO*) (Bohmert et al., 1998), *PINHEAD* (*PNH/ZWILLE*) (Moussian et al., 1998; Lynn et al., 1999; Newman et al., 2002), *FILAMENTOUS FLOWER* (*FIL*)/*YABBY* genes (Siegfried et al., 1999) and *KANADII/KANADI2* (*KANI/KAN2*) (Eshed et al., 2001; Kerstetter et al., 2001). When these genes are mutated, lateral organs frequently develop as radially symmetrical structures, demonstrating the importance of adaxial-abaxial polarity for wild-type leaf blade formation.

In response to positional cues, genes presumably dictate the process of morphogenesis by controlling both the proliferation and the differentiation of specific cell types. Studies of leaf growth in *Arabidopsis* using genetic clonal analysis (Poethig, 1985) and observation of a *cyclin1At::β-glucuronidase* (*GUS*) cell cycle reporter gene (Donnelly et al., 1999) showed that in growing leaves there is a proximal-

distal gradient of cell division rates, with the highest levels of cell division occurring in the proximal regions of the leaf. In contrast, most leaves differentiate basipetally with the distal blade forming first, followed by the proximal petiole (Poethig, 1985). Recent studies have identified a number of genes involved in the control of cell division and differentiation in lateral organs. The *LEAFY PETIOLE* (*LEP*) gene encodes an EREBP/AP2-type transcription factor that is sufficient to transform the proximally located leaf petiole into a distal blade structure (van der Graaff et al., 2000). Additional *REPRESSOR FOR LEP* (*RLP*) loci have been isolated as suppressors of an activation-tagged *lep* mutant (van der Graaff et al., 2003). Mutations in the *BLADE-ON-PETIOLE 1* (*BOP*) locus result in abnormal leaves that misexpress the meristem-promoting *knox* genes and develop numerous leaf primordia on the adaxial surface of the leaves (Ha et al., 2003). *asymmetric leaves1* (*as1*) and *asymmetric leaves2* (*as2*) mutants also misexpress *knox* genes in leaves (Byrne et al., 2000; Ori et al., 2000; Semiarti et al., 2001). Finally the *AINTEGUMENTA* (*ANT*) gene, encoding an AP2-like factor, is proposed to control organ size by regulating meristematic competence of cells within the lateral organ primordia (Krizek, 1999; Mizukami and Fischer, 2000).

We show that loss-of-function *jagged* (*jag*) mutants exhibit lateral organ defects, including narrow leaves and floral organs with serrated margins. The *JAG* locus encodes a nuclear-localized transcription factor containing a single C₂H₂-type zinc finger that is expressed exclusively in developing lateral organ primordia. When expressed ectopically, *JAG* activity is sufficient to cause cell proliferation and differentiation of leaf cell types.

Materials and methods

Plant growth conditions

Plants were grown in a (4:3:2) mixture of potting soil:vermiculite:perlite in a 22°C growth chamber with continuous cool-white fluorescent lights.

Genetic analysis of mutants

The *jag-2* and *jag-3* alleles (isolation lines, shreddie1 and shreddie2) arose in an EMS screen. Landsberg *erecta* (*Ler*) seed were mutagenized by incubation in a solution containing 0.3% (v/v) EMS (Sigma) and 0.1% (v/v) Tween 20 (Sigma) for 12 hours at room temperature. Both alleles were out crossed to wild type four times before further genetic analysis. For the construction of double mutant strains, the progeny of single mutant phenotype individuals were collected in the F₂ generation and the double mutants were observed to segregate in a 1:3 ratio in the F₃ generation. Double mutant genotypes were confirmed by polymerase chain reaction (PCR) genotyping.

Scanning electron and confocal microscopy

For SEM the inflorescence tissue was fixed and processed using a standard protocol (Bowman et al., 1989). Stages of flower development (Smyth et al., 1990) were determined. Stage 13 flowers (anthesis stage) were selected for SEM. Petals were carefully removed and mounted flat either on their adaxial or abaxial surface. For confocal analysis, 4-day post-germination seedlings were immersed in 1 mg/ml Hoechst 33342 for 1 hour. After removal of one cotyledon, seedlings were mounted in 50% glycerol under a coverslip. Tissue was imaged using a Zeiss LSM510 NLO confocal microscope equipped with a Chameleon Ti-Sapphire IR pulsed laser (Coherent) tuned to 730 nm. JAG-VENUS was detected using the 514 nm Ar laser line and a 535-590 nm band pass filter for the emitted light. Nuclear-localized Hoechst stain was detected using 730 nm excitation together with a 435-485 band pass filter for the emitted light. The two signals were collected together using multi-tracking and the images were analyzed with Zeiss LSM510 proprietary software and ImageJ (<http://rsb.info.nih.gov/ij/>).

Histology and plastic sections

Clearing of tissues for observation of vasculature by light microscopy was performed as described previously (Aida et al., 1997).

For plastic sections tissue was vacuum infiltrated with a fixation solution containing 4% paraformaldehyde, 1% glutaraldehyde and 1× phosphate-buffered saline and fixed for 12 hours at 4°C. Tissues were dehydrated stepwise in ethanol solution series. Tissues were infiltrated stepwise in Unicryl™ acrylic resin (SPI Supplies) diluted with ethanol. Samples were polymerized for 20-24 hours in a 60°C oven. Sections 0.2-2.0 μm were cut with a glass blade and a Leica RM2165 microtome. Samples were stained with 1% Toluidine Blue for 1 minute and mounted in Cytoseal-XYL (Richard-Allan Scientific).

Positional Cloning of JAG

To create a mapping population, the *jag-3* allele in *Ler* ecotype was crossed to wild-type Columbia (Col) ecotype plants. Recombinant *jag-3* mutant plants were identified in the F₂ progeny. PCR-based markers were developed for fine scale mapping using *Ler* and Col single nucleotide and insertion/deletion polymorphism sequence data located at <http://www.arabidopsis.org/Cereon/index.html>.

For genomic complementation of the mutant with genomic constructs P5112-1 and P5112-4, overlapping 10-15 kb genomic fragments spanning the BAC T26J14 were subcloned into the pPZP222 transformation vector (Hajdukiewicz et al., 1994) for transformation of *jag-3* plants by *Agrobacterium*-mediated transformation by the floral dip method (Clough and Bent, 1998). The 1.2 kb JAG cDNA was PCR-amplified from reverse transcribed *Ler* inflorescence total RNA using the primers P5.9f 5'-CCCTAGCA-

TCTCCTTCACTCAG-3' and P5.2r 5'-GGCGTTTAGACAAT-TCTAGATCTC-3'.

Generation of transgenic plants

The *JAG::VENUS* vector was generated by first PCR-amplifying a 4.6 kb genomic fragment containing the JAG promoter and coding sequences from *Ler* genomic DNA with the primers T26Bf 5'-GGATCCCGGAATAGAGCTGATGTAGTAGCCGTG-3' and T26Nr 5'-CCATGGCGAGCGAGTGATGATCTTGAACCGATTGA-3'. The gene was translationally fused to the VENUS coding sequence separated by a 10-alanine linker sequence in the transformation vector pMLBART (Gleave, 1992).

The *35S::JAG* vector was constructed by placing the JAG cDNA sequence downstream of a Cauliflower Mosaic Virus (CaMV) 35S promoter in the binary vector pCGN1547 (McBride and Summerfelt, 1990).

The *pOpL* two-component system (Moore et al., 1998) was also used to misexpress JAG. A *6XOP::JAG* expression vector was generated by first cloning the JAG cDNA downstream of six copies of the Operator sequence and an *OCS* minimal promoter in a modified version of the plasmid BJ36 (Gleave, 1992) a gift from Jeff Long (Salk Institute). The final expression cassette was in the transformation vector pART27 (Gleave, 1992). The *6XOP::JAG* construct was transformed into a transgenic driver line *pAPI::LHG4* donated by John Bowman (University of California, Davis).

In situ hybridization

In situ hybridization was performed using digoxigenin-labeled RNA probes according to a published protocol (Long and Barton, 1998). The JAG antisense probe corresponds to a 500 bp 3'-specific cDNA sequence from plasmid pJAG0.5 that was linearized with *Bam*HI and transcribed with T7 RNA polymerase, or a 1.0 kb 5'-specific cDNA from plasmid pJAG1.0 and similarly transcribed.

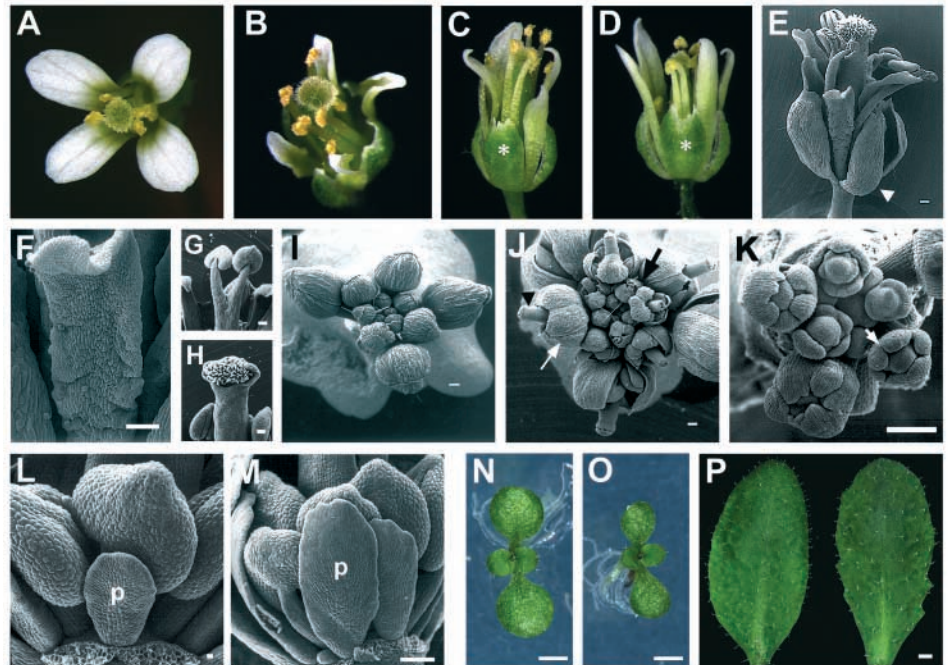
Results

The *jagged* mutation affects floral organ morphology

The *Arabidopsis* flower consists of four concentric whorls of organs that develop with distinct organ identity, position, number and size (Fig. 1A). Two ethylmethane sulphonate (EMS)-induced mutant alleles of the JAG locus were isolated in a genetic screen to identify genes that regulate floral organ morphology. The *jag-2* and *jag-3* alleles form a complementation group and overall display a similar recessive floral phenotype (Fig. 1C,D). The mutant perianth organs, sepals and petals, are narrow and 'shredded' in appearance, often with prominent jagged serrations at the distal tip of the sepal (Fig. 1B-E). The morphology of the *jag-3* stage 13 petal is characterized by adaxial curling along the margins, as well as abnormal buckling along the lateral margins of the organ (Fig. 1F) that may be an indication of uncoordinated cell growth (cell division and/or expansion). Mature *jag* petal blades also appear slightly greenish in color compared to wild-type petals. The filaments of adjacent stamens are occasionally fused along the margins and the anther is variably reduced in size and altered in shape with a pointed distal tip (Fig. 1G and data not shown). The mature *jag* carpel valves appear to bulge with seed as if there was insufficient growth of the valves as seed developed within the siliques (data not shown) and the distal stigma appears to be incompletely fused (Fig. 1H)

Scanning electron microscopy (SEM) reveals that the coordinated outgrowth of floral organ primordia is disrupted in

Fig. 1. Morphology of *jag* floral and vegetative organs. (A) Wild-type Landsberg *erecta* flower. (B,C) *jag-3* flower with narrow petals curling towards adaxial surface. Sepal with serrations at the distal tip is marked with an asterisk. (D) *jag-2* flower. (E) SEM of *jag-3* flower with a narrow sepal (arrowhead). (F) *jag-3* abaxial petal with buckled margins. (G) *jag-3* stamens fused along filament margins. (H) *jag-3* gynoecium abnormally fused at the stigma. (I) Wild-type inflorescence with sepals enclosing floral buds. (J) *jag-3* inflorescence with gynoecium protruding from floral bud (arrowhead). A wide medial sepal is present on the same flower (white arrow). A black arrow indicates a stage 7 flower with carpels protruding. (K) *jag-3* early floral primordia with an extra sepal primordium initiated (arrow). (L) Petal primordium (p) from stage 9 *jag-3* flower. (M) Petal primordium (p) from stage 10 *jag-3* flower. (N) Wild-type 7-day post germination seedling. (O) *jag-3* seedling with altered cotyledon shape. (P) Fifth rosette leaf from wild-type (left) or *jag-3* (right) that has serrated margins. Scale bar: 100 μ m (E-K,M); 10 μ m (L); 1 mm (N-P).



jag mutants. *jag-3* mutant flower buds open prematurely (Fig. 1I,J) at floral stage 7, most likely because of more rapid proximal-distal outgrowth of the carpel primordia relative to the sepal primordia that normally enclose the inner whorls of reproductive organs (Fig. 1J). Both *jag* alleles cause a slight increase in the number of sepals and petals per flower, but the third and fourth whorl organs are similar in number to the wild type (Table 1). In contrast to the single sepal present at the adaxial position of the outer first whorl in wild type, the corresponding position in *jag-3* flowers often contains either two sepals or a single wide sepal with two evenly spaced and distinct distal tips (Fig. 1D) that presumably represent either the congenital or postgenital fusion of two adjacent sepal primordia (Fig. 1J,K). Correlating with the development of extra sepals in the adaxial medial positions, an extra petal usually arises at the adaxial medial position in between the two adaxial sepals, thus giving five petals. Developing *jag-3* petal primordia are abnormal in overall shape (Fig. 1L,M) compared to wild type (Smyth et al., 1990). Specifically the distal tip of the *jag-3* petal primordium is irregular in shape and the proximal base is broadened rather than stalked.

Table 1. Floral organ numbers in *jagged* mutant alleles

Genotype	Number of sepals*	Number of petals	Number of stamens	Number of carpels
Wild type	4 \pm 0	4 \pm 0	5.85 \pm 0.03	2 \pm 0
<i>jag-2</i>	4.21 \pm 0.04	4.16 \pm 0.04	5.73 \pm 0.04	2 \pm 0
<i>jag-3</i>	4.48 \pm 0.06	4.47 \pm 0.06	5.95 \pm 0.04	2 \pm 0

The first 10 flowers were examined from 12 individual plants of each genotype.

Values are the mean \pm s.e.m. of the number of organs per whorl.

*The number of sepals completely unfused along the margins was counted.

jag mutants also displayed minor defects in vegetative organs. *jag-3* cotyledon shape is abnormal (Fig. 1O) with the petiole and blade regions more elongated than the wild-type organ (Fig. 1N). *jag* mutant rosette leaves often have mild serrations along the lateral margins, in contrast to wild type (Fig. 1P).

jag petals show defects in cell number and shape

To further characterize the *jag* perianth organ defects, petals were examined from equivalent mature anthesis stage flowers of wild-type Landsberg *erecta*, *jag-2* and *jag-3* mutants. For the comparison of the abaxial epidermal surfaces of the wild-type and *jag-2* mutant petals, the blade epidermis was equally subdivided along the proximal-distal axis into proximal, middle and distal regions containing distinct patterns of cell shape and size. The distal region in the wild-type petal contains small round epidermal cells with distinct cuticular ridges (Fig. 2A), while larger elongated cobblestone-shaped cells make up the proximal region (Fig. 2C). In the middle region of the wild-type blade, the epidermis is composed of a mixture of small round cells and cells that are both elongated in the proximal-distal axis and are intermediate in character to cells found in both the distal and proximal regions (Fig. 2B).

Adaxial epidermal cells in *jag-2* petals show the characteristic wrinkled cuticle pattern of wild-type cells (Fig. 2A,D), indicating that petal organ identity is unaffected in the *jag* mutants. However in *jag-2* mutants, there are no small round epidermal cells as in the distal region of the wild-type petal (compare Fig. 2A,D). Instead, cells located in the distal and middle regions of *jag-2* petals (Fig. 2D,E) are elongated and cobblestone-shaped and resemble cells in the proximal regions of wild-type petals (Fig. 2C). The proximal region in *jag-2* mutant petals contains larger abaxial epidermal cells that

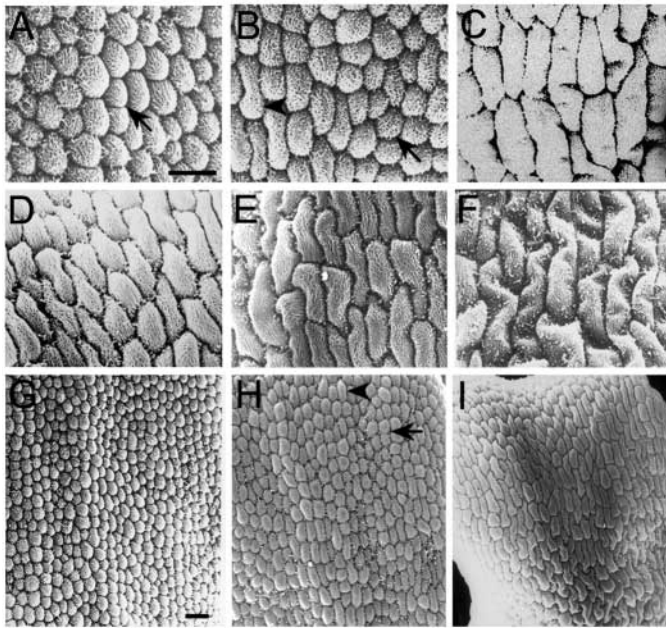


Fig. 2. SEM analysis of wild-type and *jag* mutant petals. (A,D) Distal, (B,E) middle and (C,F) proximal regions of abaxial epidermal surface. (A-C) Wild-type with (A) round epidermal cells (arrow), (B) a mixture of round (arrow) and elongated cells (arrowhead) and (C) elongated cobblestone-shaped cells (D-F) *jag-2* mutant with (D) elongated cobblestone-shaped cells, (E) elongated cells (note the fewer number of cells along proximal-distal axis than in wild type) and (F) elongated cobblestone-shaped cells. (G,H,I) The distal regions of the abaxial petal epidermis in wild-type, *jag-3* and *jag-2*, respectively, showing the allelic differences in phenotypic strength on cell shape. (H) The *jag-3* petal has both elongated (arrowhead) and round cells (arrow). (I) The *jag-2* petal only has elongated cobblestone-shaped cells. Also note a striking difference in cell numbers between wild type (G) and *jag-2* (I). For all panels distal is top and proximal is bottom. Scale bars: 20 μ m, A-F and G-I.

are more elongated than the corresponding cells in the wild-type petal (compare Fig. 2F and 2C). Because the margins of the *jag* mutant petals curl adaxially, it was difficult to flatten the organ to count the number of cells in the entire petal. Cell numbers are clearly reduced along the proximal-distal axis in the mutant (Fig. 2G,I) because the mutant epidermal cells are larger than the wild type ones. Cell numbers on the adaxial epidermal surface of the petals were similarly affected (data not shown).

The petals of *jag-3* (Fig. 2H) showed a phenotype that was weaker than that of *jag-2* (Fig. 2I), but distinguishable from wild type (Fig. 2G). Overall, the cells in the *jag-3* petal epidermis were not as elongated as in *jag-2*. The distal abaxial epidermal region of the *jag-3* petals contained a mixture of cells that were either round like wild-type distal epidermal cells, or elongated similar to those found in the *jag-2* mutant.

In summary, *jag* mutant organs are narrower and somewhat irregular in shape compared to wild-type organs. This phenotype appears to result from defects in both cell division and cell expansion from early stages in their development. Examination of *jag* petals reveals that there are fewer epidermal cells than in the wild type but that these cells are

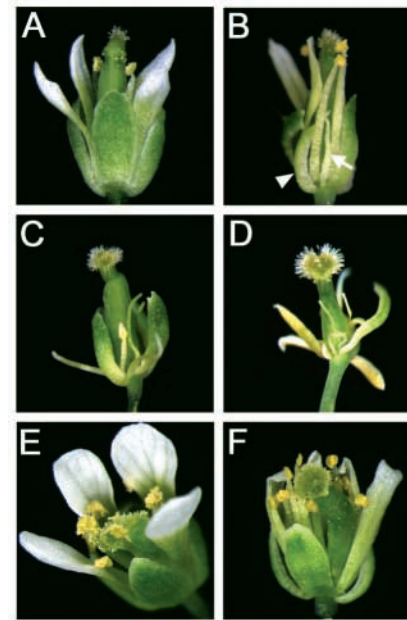


Fig. 3. Floral organ development in *jag* double mutants. (A) *ant-9* flower with narrow organs. (B) *ant-9 jag-3* flower with narrow reduced floral organs. Sepal (arrowhead) and petal (arrow). (C) *fil-1* flower. (D) *fil-1 jag-3* flower. (E) *sup-5* flower. (F) *sup-5 jag-3* flower.

larger than normal. This in turn suggests that *jag* cells are not restricted in their ability to expand but instead are unable to divide as rapidly.

***jag* double mutants with genes involved in lateral organ development**

The phenotype of *jag* mutants closely resembles that of the *aintegumenta* (*ant*) mutant. *ANT* regulates growth and cell division in floral organ primordia and ovules (Elliott et al., 1996; Klucher et al., 1996). To determine if there could be an overlap in the function of these two genes, double mutant plants were generated with the strong loss-of-function *ant-9* allele. *jag-3 ant-9* double mutant plants display a phenotype that is much more severe than either single mutant in that floral organs become reduced narrow structures that fail to elongate to the same extent as in either single mutant (Fig. 3A,B). This enhanced phenotype suggests that both *ANT* and *JAG* may function in parallel pathways that contribute to floral organ size and shape.

The *filamentous flower* (*fil*) mutant also produces narrow perianth organs (Fig. 3C) (Chen et al., 1999; Kumaran et al., 1999; Sawa et al., 1999). *FIL* is a key regulator of adaxial/abaxial patterning in lateral organs and functions redundantly with other members of the *YABBY* gene family (Siegfried et al., 1999). Double mutants between *jag-3* and *fil-1*, a strong *fil* allele, have an additive floral phenotype (Fig. 3C,D). Numerous filamentous organs are produced in the place of petals and stamens in the double mutants. *jag-3 fil-1* double mutant flowers have slightly narrower sepals in the first whorl compared to the single mutants, and in the fourth whorl the gynoecium has an elongated styler region and a reduced carpel valve. These gynoecium abnormalities are observed in *fil* mutants and have been interpreted as a defect in proximal-

distal patterning in the floral primordium (Chen et al., 1999). Thus, the overall additive phenotype indicates that *JAG* acts independently of *FIL* and is therefore unlikely to function in patterning adaxial/abaxial organ polarity.

The *SUPERMAN* (*SUP*) gene is involved in regulating stamen and carpel development and floral organ number, possibly via the control of cell proliferation within the flower (Bowman et al., 1992; Sakai et al., 1995). Double mutant flowers harboring the null *sup-5* allele and *jag-3* displayed a completely additive phenotype characterized by *jag-3* petal and sepal morphology, and increased stamen number and unfused carpel tissues similar to that observed in the *sup-5* single mutant phenotype (Fig. 3E,F). These data indicate that *JAG* and *SUP* function independently in the processes of organ growth and organ number determination in the flower. *clavata3* (*clv3*) mutants exhibit enlarged meristems and increased organ number in all floral whorls (Brand et al., 2000; Fletcher et al., 1999). *clv3 jag* double mutants also show an additive phenotype (data not shown) suggesting that *JAG* does not interact with other meristem genes of the *CLAVATA* signaling pathway involved in maintenance of cell proliferation in the shoot and floral meristem.

***JAG* is required for bract outgrowth in *leafy*, *apetala1* and *apetala2* mutants**

The *leafy* (*lfy*) mutant produces flowers with only leaf-like organs, and bracts or floral leaves are produced at the base of each pedicel/peduncle (Fig. 4A) (Weigel et al., 1992). In *lfy-6 jag-3* double mutants, the bract-like organs that develop at the base of the floral pedicel/peduncle are much reduced compared to *lfy-6* single mutants and are frequently filamentous (Fig. 4B-D). The partial loss-of-function *lfy-5* allele results in a less severe phenotype in the flower compared to *lfy-6* that consists of bract-like sepals in the outer whorl and a slight reduction in petal and stamen formation in the inner whorls. Flowers mutant for both *lfy-5* and *jag-3* display characteristics associated with both single mutant, but the bract-like sepals in the lateral positions fail to grow out (compare Fig. 4E and F) and are often replaced with small projections. Occasionally, a few flowers lack outgrowth of all four bract-like sepals (data not shown). Flowers of *lfy-6 jag-3* double mutants also appeared to produce fewer organs than the total number of floral organs produced in either single mutant, and they are arranged in a spiral pattern (data not shown). Thus, *JAG* is required for bract outgrowth both at the base of pedicels/peduncles and in the flowers in the *lfy* mutant background.

Bract-like sepals are also formed in the first whorl of 'A function' floral organ identity mutants such as *ap1-1* and *ap2-1* (Bowman et al., 1993; Bowman et al., 1991). To determine if *JAG* is also necessary for bract development in the flower, double mutant combinations were made. The *ap1-1 jag-3* double mutant flowers produced fewer first whorl bract-like sepals than *ap1-1* single mutants (Fig. 4I,J) in the early arising flowers after the transition to reproductive development. Similarly, the bract-like sepals of *ap2-1* mutants failed to grow out, usually in the lateral positions, in *ap2-1 jag-3* double mutant flowers (Fig. 4G,H), but sometimes all four first whorl organs failed to grow out (data not shown).

In summary, *JAG* is necessary for normal outgrowth of floral bract-like organs in the first whorl of *lfy-5*, *ap1-1* and *ap2-1*

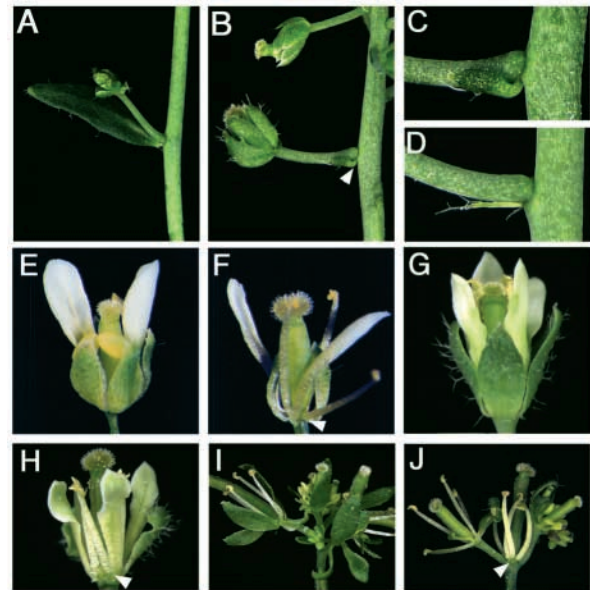


Fig. 4. Phenotypes of double mutants between *jag* and bract forming mutants, *lfy*, *ap2* and *ap1*. (A) Bract subtending a *lfy-6* flower. (B) Reduced bract forms at the base of *lfy-6 jag-3* flower (arrowhead). (C,D) Close-up image of a *lfy-6 jag-3* reduced bract (C) and a filamentous structure (D). (E) *lfy-5* flower with lateral and medial sepals. (F) *lfy-5 jag-3* flower with lateral first whorl organs missing (arrowhead). (G) *ap2-1* flower with bract-like sepals. (H) *ap2-1 jag-3* flower with lateral first whorl organs missing (arrowhead). (I) *ap1-1* inflorescence with bract-like sepals. (J) *ap1-1 jag-3* inflorescence with reduced numbers of bract-like sepals (arrowhead).

flowers, in addition to having a role in outgrowth of all four floral organs in the wild-type flower.

Positional Cloning of *JAG*

The position of the *JAG* locus was determined by its genetic linkage to BAC-specific molecular markers corresponding to Landsberg *erecta* and Columbia ecotype sequence polymorphisms using a recombinant F₂ mapping population representing 856 chromosomes (Fig. 5A). Fine-scale mapping analysis revealed that *JAG* is located on BAC clone T26J14. Two independent overlapping 10 kb genomic fragments corresponding to BAC T26J14 sequences when transformed into plants rescued the *jag-3* mutant phenotype (data not shown). Sequencing of candidate genes encoded by this genomic region in the *jag-2* and *jag-3* mutants revealed nucleotide sequence changes in the gene At1g68480. The *JAG* gene sequence was defined by genetic complementation to encompass a 4.5 kb genomic fragment and the coding exons were found to be interrupted by 5 introns. A cDNA sequence 1177 base pairs (bp) in length that is in agreement with a 1.2 kb transcript detected by northern blot (data not shown) was obtained from an inflorescence cDNA population.

The *JAG* locus encodes a 248 amino acid protein with motifs that suggest a role as a transcription factor (Fig. 5B). *JAG* belongs to a large family of C₂H₂-type zinc finger transcription factors that contains 112 members in *Arabidopsis* (Riechmann, 2002). *JAG* contains a single 31 amino acid single C₂H₂-type zinc finger motif (amino acid positions 51-81) that may have a function in

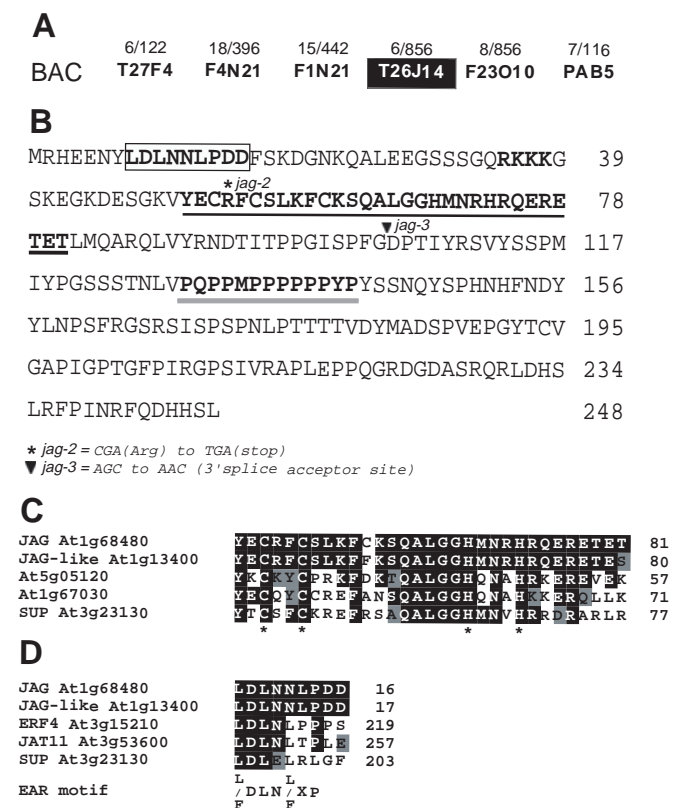


Fig. 5. Map-based cloning and sequence of *JAG*. (A) Schematic of positional cloning of the *JAG* locus showing the frequency of recombinant chromosomes identified in a mapping population with respect to molecular markers corresponding to BAC clones. Fine-scale mapping localized the *JAG* locus to the BAC T26J14 (black box). (B) Amino acid sequence of the *JAG* protein. Positions and nature of the *jag-2* (asterisk) and *jag-3* (black arrowhead) mutations are indicated. The EAR repression motif is boxed. A putative nuclear localization sequence is shown in bold font. The single C₂H₂-type zinc finger motif is underlined in black. A proline-rich motif is underlined in gray. (C) Amino acid alignment of the *JAG* C₂H₂ zinc finger domain with other *Arabidopsis* proteins. The positions of conserved cysteine and histidine residues involved in coordinating a zinc ion are indicated by asterisks. (D) Amino acid alignment of the *JAG* EAR repression motif with other *Arabidopsis* proteins. The EAR repression consensus motif is indicated below. Identical residues are in black boxes; similar residues in gray boxes.

DNA binding. A BlastP sequence search and alignment of the *JAG* zinc finger motif with other related *Arabidopsis* proteins reveals that *JAG* is closely related in sequence to the protein At1g13400 or *JAG-like* (29/31 identical amino acids in the zinc finger) while the proteins At5g05120, At1g67030 and SUPERMAN (SUP), have 19/31, 16/31 and 16/31 identical amino acids in the zinc finger, respectively, and are less closely related (Fig. 5C). All plant C₂H₂-type zinc finger proteins, including *JAG*, contain a conserved QALGGH sequence that has been shown in the SUP zinc finger to form part of an alpha-helix that contacts the major groove of DNA (Isernia et al., 2003).

Other motifs identifiable in the amino terminus of the *JAG* protein sequence include a putative nuclear localization sequence at position 35-38 and a short nine amino acid ERF-associated amphiphilic repression (EAR) motif (position 8-16)

(Ohta et al., 2001). The repressor activity of the EAR motif has been demonstrated for the plant transcription factors ERF4 and JAT11 (Ohta et al., 2001) and for SUP where it has been shown to have a repressor function in vivo (Hiratsu et al., 2002). The *JAG* EAR motif contains three out of nine leucine residues and shows amino acid sequence conservation in an alignment with similar motifs present in previously characterized zinc finger transcription factors (Fig. 5D). Similarly to the SUP protein, *JAG* contains a proline-rich motif located at amino acids 129-141 in its carboxyl terminus that may function in transcriptional repression or activation. Taken together, the presence of these functional domains suggests that *JAG* is a nuclear-localized repressor of transcription.

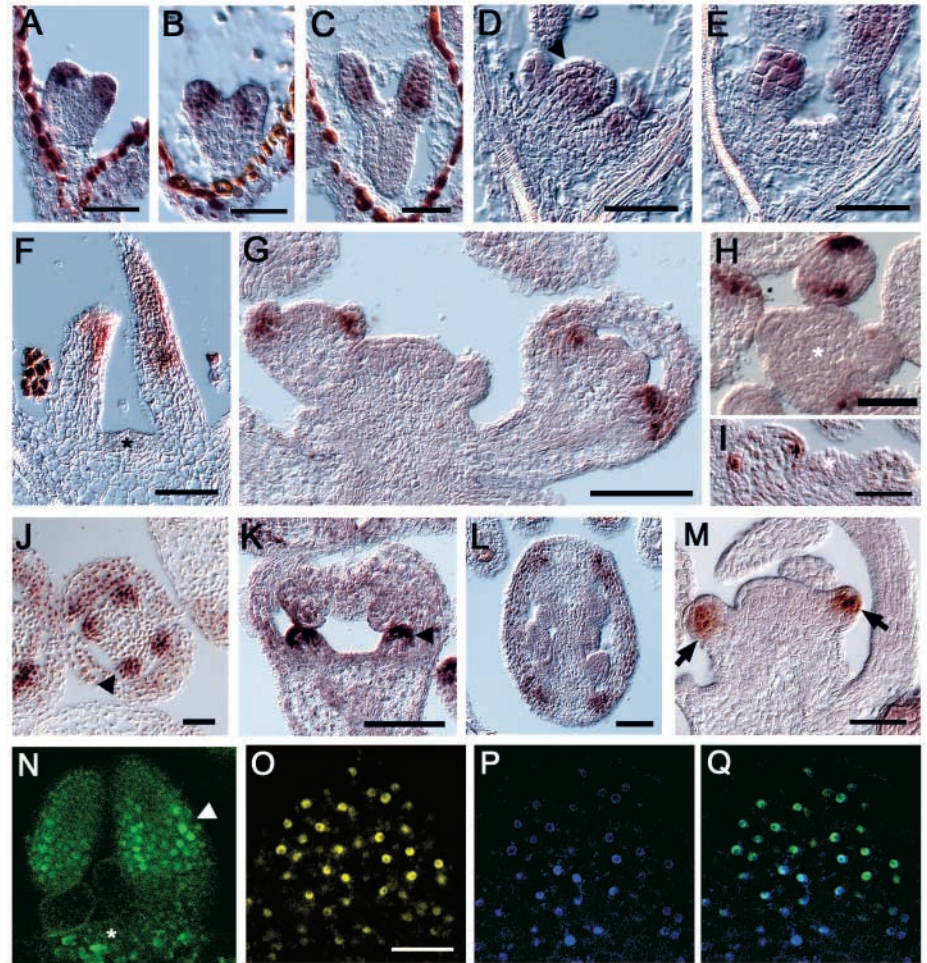
The *jag-2* mutation results in a premature stop codon at residue 54 at the start of the zinc finger motif, while the *jag-3* mutation disrupts the 3'-splice acceptor sequence in the fourth intron, resulting in the production of a slightly larger transcript on northern blots (data not shown) and a predicted protein that is truncated at residue 104 with the addition of 11 extra amino acids. Consistent with the identified DNA lesions, the *jag-2* allele is phenotypically slightly more severe than the *jag-3* allele, according to our analysis of abaxial petal epidermis, and represents a stronger loss-of-function allele.

***JAG* is expressed in lateral organ primordia and encodes a nuclear localized protein**

The developmental pattern of *JAG* mRNA localization was determined by in situ hybridization. *JAG* mRNA is first detected in late transition stage embryos in cells corresponding to the cotyledon primordia. *JAG* transcripts are uniformly localized throughout the newly emerging cotyledon primordia but are absent from the SAM (Fig. 6A). As the cotyledon primordia continue to grow out during the heart stage, *JAG* mRNA expression is excluded from the tips of the cotyledon primordia but continues to be expressed in a band below this region of repressed expression (Fig. 6B). In the torpedo stage embryo, *JAG* expression continues to be absent at the tip of the cotyledon primordia (Fig. 6C). Cells in the epidermis of the cotyledon have a lower level of *JAG* transcripts than cells in the inner layers. *JAG* is also expressed in developing leaf primordia of the seedling at 3.5 days and/until 7 days after germination. It is initially expressed throughout the young primordium but later expression becomes excluded from the distal tip of the primordium (Fig. 6D-F). Reduced *JAG* expression is also detected at the proximal base of the leaf primordia (Fig. 6F). After the transition to reproductive development, *JAG* transcripts are absent in the inflorescence meristem but are detected in developing floral organ primordia (Fig. 6G). During flower development *JAG* transcripts are first detected in stage 3 flowers in sepal anlagen (Fig. 6H,I). Expression in the medial sepals precedes expression in the lateral sepals that are later to develop (Fig. 6H,I and data not shown). A lower level of transcripts is detected at the distal tip of the sepal primordia of stage 4 flowers and onwards (Fig. 6G). Expression in the sepals decreases in stage 6-8 flowers and transcripts are detected in stamen and petal primordia, but expression is slightly reduced at the base of these primordia (Fig. 6G,J,K). Some *JAG* transcripts are detected in stage 8 carpel primordia (not shown) as well as in carpel valves in transverse sections of stage 9 gynoecia (Fig. 6L).

Lastly, we examined *JAG* expression in *lfy-6* inflorescences

Fig. 6. Expression pattern of *JAG*. (A-L) RNA localization by in situ hybridization with *JAG* antisense probe. (A) Late transition stage embryo. (B) Heart stage embryo. (C) Torpedo stage embryo. (D) and (E) Consecutive longitudinal section through a seedling 3.5 days after germination. (F) Seedling 7 days after germination. (G) Longitudinal section of inflorescence meristem and early floral buds. (H) Transverse section of inflorescence meristem. (I) Expression in stage 3 floral bud. (J) Transverse section of stamen primordium of stage 6 flower. (K) Stage 8 petal primordium (arrowhead) longitudinal section. (L) Transverse section of stage 10 gynoecium. (M) Inflorescence of *lfy-6* mutant with *JAG* expression in early bract primordia (arrows). (N) Confocal optical section showing the *JAG::VENUS* transgene expressed in seedling 4 days after germination. Nuclear expression of the fusion protein is confined to the growing region (arrowhead) of the leaf primordium. (O) *JAG*-*VENUS* subcellular localization (yellow) in cells of a leaf primordium. (P) Hoechst 33342 nuclear staining (blue). (Q) Merged image of O and P showing nuclear co-localization (green). Meristem is indicated by asterisk in some panels. Scale bar: 100 μ m (G,K); 30 μ m (O-Q); 50 μ m in all other panels.



since the *lfy-6 jag-3* double mutant phenotype indicated that *JAG* activity is important for *lfy* bract outgrowth. We found that in *lfy-6* inflorescences *JAG* expression is detected in bract primordia (Fig. 6M) however, we were unable to detect transcripts in a domain within the inflorescence meristem corresponding to a bract anlagen.

To determine the subcellular localization of the *JAG* protein, a 4.5 kb genomic fragment containing putative 5'-regulatory sequences plus the *JAG* coding sequences was translationally fused to *VENUS*, a rapidly maturing variant of Yellow Fluorescent Protein (Nagai et al., 2002). The transgene was expressed in *jag-3* plants and completely rescued the mutant phenotype in 15 out of 17 T₁ plants, indicating that the fusion protein was functional in plants (data not shown). The expression of the fusion protein mimicked the *JAG* RNA localization pattern as observed by in situ hybridization. Confocal laser scanning microscopy of a seedling at 4 days after germination shows the *JAG*-*VENUS* protein within the leaf primordium in a distinct band of expression (Fig. 6N). In leaf primordium cells, the *JAG*-*VENUS* protein co-localizes with Hoechst 33342 nuclear staining (Fig. 6O-Q). Consistent with the predicted protein function and the presence of a consensus nuclear localization sequence (Fig. 5B), the *JAG*-*VENUS* fusion protein is located in the nucleus.

In summary, *JAG* transcripts are exclusively localized to all lateral organ primordia throughout the plant, where expression

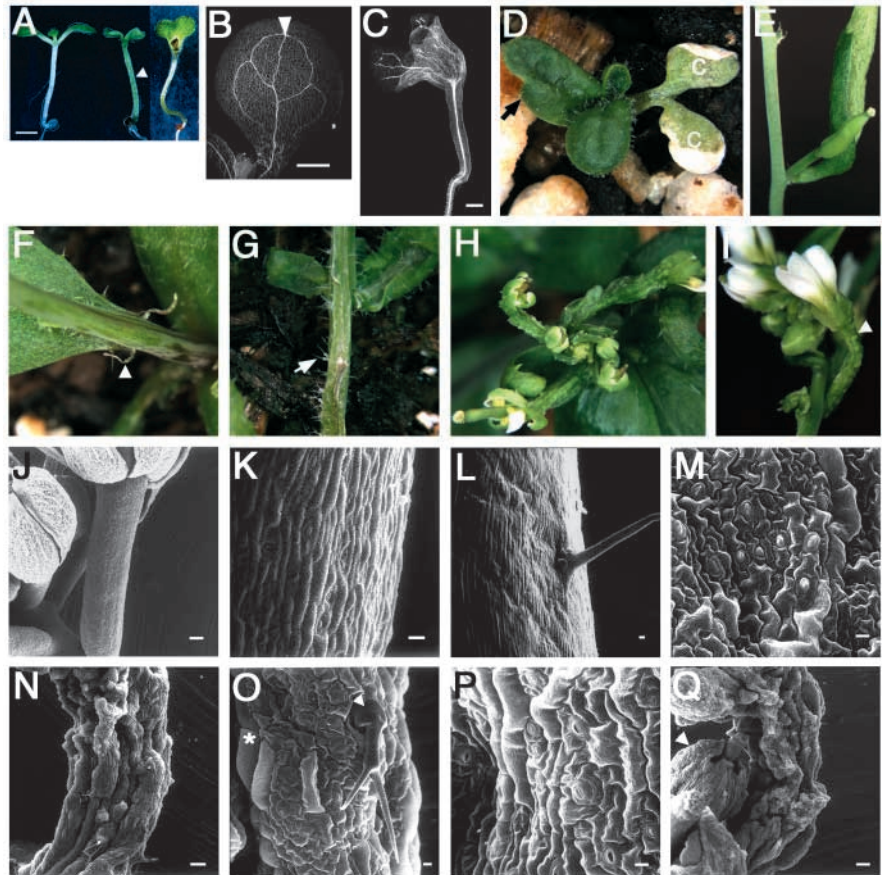
is at first uniform throughout the young emerging primordia and then absent from the distal tips of organ outgrowth.

***JAG* misexpression is sufficient for development of leaf-like tissues**

Since *JAG* is necessary to promote lateral organ growth, we tested whether *JAG* activity is sufficient for such growth by expressing it constitutively. A *35S::JAG* construct expressed in both wild-type and *jag-2* mutant backgrounds resulted in similar phenotypes. Detailed analysis of transgenic lines is described in the wild-type background. *35S::JAG* transgenic plants showed disrupted organogenesis and the formation of ectopic leaf-like tissues throughout the plant.

The abnormal phenotype was first noted at the seedling stage. *35S::JAG* hypocotyls often appeared green in color, in contrast to wild-type hypocotyls that are yellowish and lack high levels of chlorophyll (Fig. 7A). In addition, varying degrees of cotyledon fusion (44 out of 104 T₁ plants) were observed, including either a single fused cotyledon or a goblet-shaped structure resulting from fusion along both lateral cotyledon margins (Fig. 7A). These seedlings were cleared using chloral hydrate to allow examination of the vasculature. In the wild-type cotyledons, the vasculature consists of a central midvein that runs along the proximal-distal axis and a small number of secondary veins that branch off from it (Fig. 7B). *35S::JAG* cotyledons exhibit a highly irregular

Fig. 7. *35S::JAG* Misexpression. (A) Wild-type (left) and *35S::JAG* (middle and right) seedling phenotypes, the latter with greening of hypocotyl (arrowhead) and variable fusion of cotyledons. (B) Vasculature of wild-type cotyledon. Arrowhead indicates midvein. (C) Vasculature of *35S::JAG* fused cotyledons shows no obvious midvein. (D) to (I) *35S::JAG* vegetative and floral defects. (D) Fusion of rosette leaves (arrow) and cotyledon (c) fusion along the petiole margins. (E) Bract formation at the base of the flower pedicel. (F) Stipule outgrowth from the lateral margins at the base of the leaf (arrowhead). (G) Growth of leaf-like tissue and stellate trichomes (arrowhead) on the stem. (H) Abnormal flowers emerging from the inflorescence. (I) Flower with fused sepals connected to abnormal pedicel (arrowhead). (J-Q) SEM analysis of wild-type pedicel (J,K), stem with trichome (L), and leaf with pavement cells (M) in comparison to *35S::JAG* pedicel (N,O,Q) and *35S::JAG* stem (P). *35S::JAG* pedicel cell types resemble leaf pavement cells. Trichome (arrowhead) and large petal-like cell (asterisk) are indicated in O. Fusion between adjacent sepals (arrowhead) is indicated in Q. Scale bars 1 mm (A); 500 μ m (B); 200 μ m (C); 100 μ m (J,N,Q); (K), (L), (M), (O), (P) 10 μ m (K-M, O, P).



vasculature in which a central midvein is not identifiable and the strands do not form a closed circuit (Fig. 7C). Many *35S::JAG* seedlings also fail to develop leaves after germination. In those that do, the leaves are often irregular in shape and adjacent leaves may be fused along the lateral margins (Fig. 7D). During reproductive stages some of these plants develop a bract from the base of the flower pedicel similar to *lfy* mutants (Fig. 7E). Unusual outgrowth of stipules is also observed from the base of leaves (Fig. 7F).

Ectopic leaf-like tissue appears to develop on many surfaces throughout the plant, and its location is not confined by wild-type organ boundaries (Fig. 7G-Q). Stellate trichomes, normally found on the adaxial surface of leaves, are numerous on the surface of the abnormal *35S::JAG* stems and pedicels (Fig. 7G,O). The epidermis of pedicels and stems was examined by SEM. In contrast to the wild-type pedicel and stem that have regular files of rectangular epidermal cells (Fig. 7J-L), the pedicels and stems of *35S::JAG* plants are larger in diameter and consist of abnormal cell types that resemble stellate trichomes and leaf pavement cells, as well as cell types that are unrecognizable but contain cuticular ridges resembling those found on petal epidermal cells (Fig. 7N-P). Both *35S::JAG* pedicel (Fig. 7O) and stem (Fig. 7P) epidermis contain cells that closely resemble leaf pavement cells (Fig. 7M). The leaf-like outgrowths on the *35S::JAG* pedicels extend to the flower sepals (Fig. 7H,I) where lateral margins of adjacent sepals become fused (Fig. 7I,Q). Petals, stamens and carpels of the *35S::JAG* flowers develop normally or as reduced structures.

To further characterize the sub-epidermal structure of these ectopic leaf-like tissues, the internal anatomy of *35S::JAG* stem tissue was analyzed. Transverse sections of *35S::JAG* stems reveal that the morphology of the centrally located pith cells, surrounding cortex and vascular bundles, containing xylem and phloem, is similar to that of the corresponding tissues in the wild type (Fig. 8A,B). However, numerous finger-like projections of tissue are found to emanate from the cortex and epidermal regions (compare Fig. 8A and B). Closer examination of cell types contained in these finger-like outgrowths reveals a striking resemblance to the structure of the wild-type leaf (Fig. 8C). There are large epidermal cells of variable size on the surfaces of the *35S::JAG* stem outgrowths, which resemble pavement cells found in the wild-type leaf epidermis (compare Fig. 8C,D), while the subepidermal layer contains cells that are irregular in shape and size (Fig. 8D) and have a resemblance to the palisade and spongy mesophyll cell types found in leaves (Fig. 8C). A vascular bundle containing phloem and xylem cells was found to run through one of the finger-like outgrowths from the *35S::JAG* stem and the cells that abut the xylem cells are elongated and have the morphology of the palisade mesophyll, whereas cells that abut the phloem cells are smaller and have the morphology of the spongy mesophyll (Fig. 8F). Some finger-like projections contain vascular tissue and appear to have normal leaf adaxial-abaxial patterning, while others lack the vasculature and organized tissue structure. Overall the cell types found in the finger-like outgrowths of the *35S::JAG* stem resemble cell

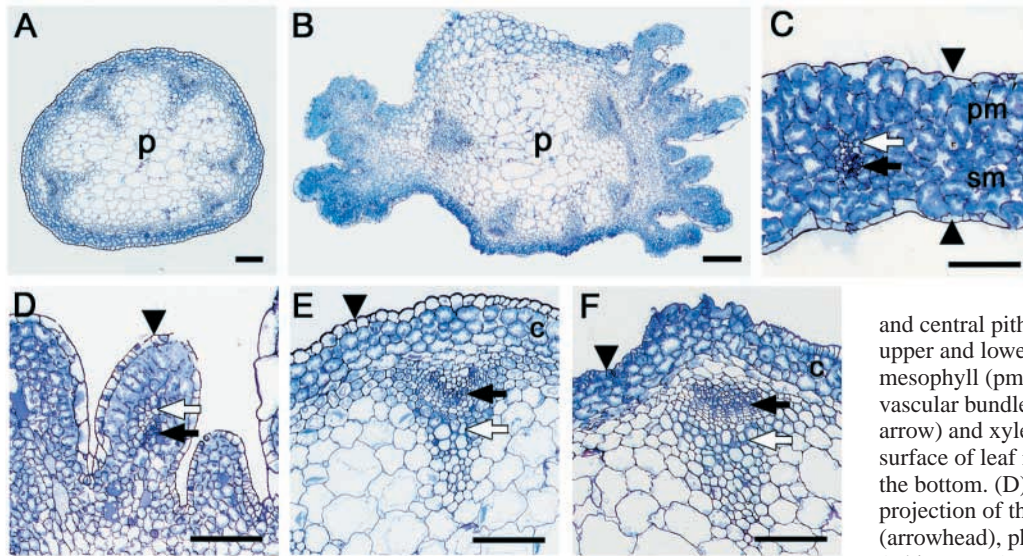


Fig. 8. Transverse sections of stem and leaf showing vegetative structure. (A) wild-type stem with central pith (p). (B) *35S::JAG* stem is larger in diameter than wild type with numerous finger-like projections

and central pith (p). (C) Wild-type leaf showing upper and lower epidermis (arrowheads), palisade mesophyll (pm), spongy mesophyll (sm) and vascular bundle composed of phloem cells (black arrow) and xylem cells (white arrow). Adaxial surface of leaf is at the top and abaxial surface is at the bottom. (D) Close-up image of finger-like projection of the *35S::JAG* stem with epidermis (arrowhead), phloem (black arrow) and xylem (white arrow). (E,F) Region of wild-type (E) and

35S::JAG (F) stem with outer epidermis (arrowhead), cortex (c), phloem (black arrow) and xylem (white arrow). Scale bar: 100 μ m (A); 200 μ m (B); 100 μ m (C-F).

types found in leaves. Regions of the stem that lack visible leaf-like projections do however show abnormalities in the epidermis and cortex. The wild-type stem epidermis is composed of a single layer of small regular cells and the cortex is composed of about three cell layers of uniformly sized round cells (Fig. 8E). In contrast, the *35S::JAG* stem epidermal and cortical cells are variable in size and irregular in shape. (Fig. 8F).

Development of leaf-like tissues in place of flowers by *JAG* misexpression

Since the constitutive *35S::JAG* transgene resulted in a severe seedling phenotype that could obscure a floral gain-of-function phenotype, a two-component system (Moore et al., 1998) was used to express *JAG* under the control of the *API* promoter. A driver transgenic line *pAPI::LhG4* containing the *API* promoter drives expression of the chimeric LhG4 transcriptional activator. When combined with an *OP::GUS* reporter gene in double transgenic plants, this *pAPI::LhG4* driver results in a GUS staining pattern that mimics the *API* expression pattern (data not shown). A *6XOP::JAG* transgene was transformed into the *pAPI::LhG4* driver line. 23 out of 25 T₁ plants developed normally until the transition to flowering, when *API* is first expressed throughout the stage 1 floral primordium (Mandel et al., 1992). Flower development was completely inhibited in *pAPI::LhG4 6XOP::JAG* plants. Instead leaf-like structures, pedicels with leaf-like outgrowths, or radially symmetric or club-shaped structures developed (Fig. 9A). Similar pedicels with leaf-like tissues were observed in *35S::JAG* plants (Fig. 7H,I). Although a cup-like receptacle structure formed at the distal end of some mature *pAPI::LhG4 6XOP::JAG* pedicels (Fig. 9B), no floral organs developed. We conclude that misexpression of *JAG* in the floral meristem is sufficient to promote growth of leaf-like tissues in the place of flowers, and thereby override normal floral organ development.

Discussion

JAG promotes growth of leaf tissues

Our study has uncovered a novel gene involved in lateral organ development. While *JAG* is not essential for the initiation of leaf primordia, it is required for the coordination of cell division and expansion during organ morphogenesis, and its expression, being limited to developing organ primordia, suggests that it functions directly in this process. However the *jag* phenotype is relatively mild compared to many other mutations affecting leaf development including *fil/yabby* (Siegfried et al., 1999), *phab* (McConnell and Barton, 1998) and *pnh/zwille* (Moussian et al., 1998; Lynn et al., 1999; Newman et al., 2002). It is therefore surprising that *JAG* misexpression appears capable of inducing the proliferation of leaf-like tissue in a variety of contexts. These observations suggest that perhaps the weak *jag* loss-of-function phenotype may be the result of genetic redundancy. One promising candidate is the *JAG-like* gene At1g13400 as it is the most closely related gene in the *Arabidopsis* genome and contains nearly identical C₂H₂ zinc finger and EAR repression motifs. Our preliminary analysis indicates that the expression pattern of At1g13400 overlaps with *JAG* in lateral organs and we are currently investigating loss-of-function double mutants (C.K.O. and E.M.M., unpublished).

The *jag* loss-of-function mutant shares some similarities in phenotype with two recently characterized mutants *cincinnata* (*cin*) and *jaw*. The *Antirrhinum majus CIN* gene encodes a TCP DNA binding factor that is involved in control of leaf shape and curvature by regulating cell cycle arrest in the distal region of the growing leaf (Nath et al., 2003). A similar leaf growth phenotype is associated with the activation-tagged mutant *jaw*. *JAW* encodes a microRNA similar in sequence to the *Arabidopsis TCP4* gene and has been shown to negatively regulate *TCP4* (Palatnik et al., 2003). Like *jag* petals, both *cin* and *jaw* mutant leaves are buckled along the margins. Furthermore, both *TCP4* and *JAG* are normally expressed in

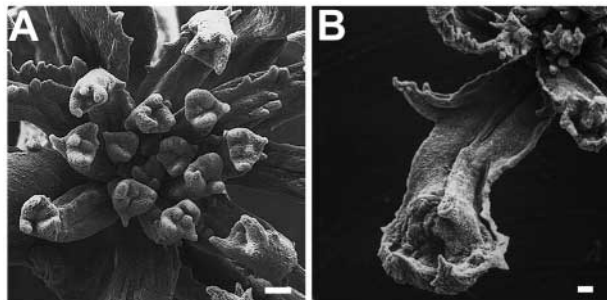


Fig. 9. Misexpression of *JAG* in flowers with *pAPI:LhG4 6XOP::JAG*. (A) Inflorescence with variable leaf-like organs in place of flowers. Organs are club-shaped with leaf-like pedicels after the transition to reproductive development. (B) A mature leaf-like organ. Scale bar: 100 μ m.

growing leaf primordia and their misexpression leads to seedlings with fused cotyledons suggesting that in *Arabidopsis* *TCP4* and *JAG* may function in similar pathways regulating leaf growth.

JAG encodes a nuclear localized putative transcriptional repressor that therefore might repress an inhibitor of leaf growth. One candidate repressor of leaf growth is the *BLADE-ON-PETIOLE 1 (BOP)* gene. The *bop* mutant is characterized by the development of ectopic leaf tissues in the form of primordia on the proximal adaxial surfaces of the cotyledons and leaves, and ectopic expression of the *knox* genes, *KNAT1*, *KNAT2* and *KNAT6* (Ha et al., 2003). The proposed *BOP* function is to control leaf morphogenesis by repressing meristematic growth and differentiation in the proximal region of the leaf.

JAG, cell division and *ANT* function

JAG shows a dynamic pattern of transcript localization that is restricted to growing lateral organ primordia. At the onset of organ primordium outgrowth *JAG* mRNA is localized throughout the primordium, but soon becomes restricted to a smaller domain as it is excluded from the distal tip. This expression pattern is similar to that of a *cyclin1At::GUS* cell cycle reporter gene that is also down-regulated in the distal end of developing leaf primordia (Donnelly et al., 1999). Thus, *JAG* expression appears to coincide with regions undergoing active cell division and may be causal in this process. A close examination of the narrow *jag* petals, revealed that the *jag* petal epidermis contains fewer cells along the proximal-distal axis, thereby implicating a *JAG* function in cell division control. The subdomain of *JAG* expression at the distal petal tip in early stage primordia provides patterning to the proximal-distal axis and may help to set up a gradient of petal epidermal cell sizes encountered along the proximal-distal axis that appears to be altered by loss of *JAG* activity. *ANT* function is also associated with cell division and organ growth, and the *ant jag* double mutant phenotype is consistent with the two genes having similar functions. However, unlike *JAG*, overexpression of *ANT* results in normally shaped, albeit enlarged, organs (Krizek, 1999; Mizukami and Fischer, 2000). Thus, *JAG* and *ANT* are unlikely to affect the same target genes when ectopically expressed.

JAG and bract formation

While bract formation is suppressed in *Arabidopsis* (Hempel and Feldman, 1994) and other members of the *Brassicaceae* family, a cryptic bract has been proposed to exist in *Arabidopsis* based on the expression of *ANT* in the inflorescence meristem as well as the complimentary expression of *STM* (Long and Barton, 2000). The expression of *FIL* and *ASI* in a similar domain to that of *ANT* further supports this proposal (Byrne et al., 2000; Long and Barton, 2000; Siegfried et al., 1999). *JAG* is exceptional in this respect in that it is an early leaf development gene that is not expressed in the cryptic bract. Since constitutive expression of *JAG* is sufficient for the outgrowth of floral bracts, loss of *JAG* activity in the cryptic bract may be responsible in part for the absence of bracts in the *Brassicaceae* family. Consistent with this proposal, *JAG* is expressed in *lfy* mutant bracts and is required for their proper development.

A JAG-specific pathway of leaf tissue growth

Analysis of the *phan* mutant in *Antirrhinum*, led Waites and Hudson to propose that blade outgrowth requires the juxtaposition of adaxial and abaxial boundaries (Waites and Hudson, 1995; Waites et al., 1998). This model has been subsequently supported by studies of the organ polarity genes *FIL*, *KAN1/KAN2*, *PHB*, *PHV*, *AGO* and *PNH/ZWILLE* in *Arabidopsis* [summarized by Bowman et al. (Bowman et al., 2002)]. Given that *JAG* is the only gene known to be sufficient to promote growth of leaf tissue, it is important to determine whether *JAG* normally acts in response to such boundaries or whether it may promote boundary formation. In regard to this question it is worth noting that the *JAG* gain-of-function phenotype is sensitive to the context of the plant cellular environment, in that the phenotype produced by gain-of-function *JAG* in any particular cell depends on the tissue in which it is expressed. For instance, although ectopic *JAG* expression results in regularly shaped floral bracts, the leaf-like tissue that develops from the stem appears disorganized and lacks any overall leaf-like shape. Hence patterning information appears to be largely absent although specific cell types associated with adaxial and abaxial leaf domains are present and are sometimes observed to be arranged in an organized manner. *JAG* expression, although occurring early in leaf development, also appears to be initiated slightly later than that of genes such as *PHAB* or *FIL*, supporting a role for *JAG* downstream of adaxial-abaxial boundary production. Although our genetic analysis of the *fil-1 jag-3* double mutant suggests that *JAG* and *FIL* act in different pathways, in both cases genetic redundancy of *JAG* with *JAG-like* and *FIL* with *YABBY3/YABBY2* (Siegfried et al., 1999) may mask the participation of the individual genes in organ growth and abaxial polarity specification. We therefore favor the proposal that *JAG* normally acts downstream of leaf patterning genes during lateral organ development, in order to promote the wild-type pattern of cell division and differentiation. It will be interesting to try to separate these *JAG*-specific functions by identifying the downstream targets of *JAG* gene activity.

We thank Jennifer Li and Stefan Wenkel for valuable assistance with positional mapping analysis, John Bowman for providing plant lines, and Marcio Alves Ferreira, Catherine Baker, Pradeep Das,

Annick Dubois, Liz Haswell, Toshiro Ito, Jeff Long, Patrick Sieber, Frank Wellmer, and Hao Yu for critical comments on the manuscript. We also thank José Dinneny and Detlef Weigel for coordinating their publication with ours. C.O. received a postdoctoral fellowship from NSERC and G.V.R. is a fellow of the Jane Coffin Childs memorial fund for medical research. This work was supported by US National Science Foundation grant IBN-0211670 to E.M.M.

References

- Aida, M., Ishida, T., Fukaki, H., Fujisawa, H. and Tasaka, M. (1997). Genes involved in organ separation in *Arabidopsis*: an analysis of the cup-shaped cotyledon mutant. *Plant Cell* **9**, 841-857.
- Bohmert, K., Camus, I., Bellini, C., Bouchez, D., Caboche, M. and Benning, C. (1998). *AGO1* defines a novel locus of *Arabidopsis* controlling leaf development. *EMBO J.* **17**, 170-180.
- Bowman, J. L., Alvarez, J., Weigel, D., Meyerowitz, E. M. and Smyth, D. R. (1993). Control of flower development in *Arabidopsis thaliana* by *Apetalal* and interacting genes. *Development* **119**, 721-743.
- Bowman, J. L., Eshed, Y. and Baum, S. F. (2002). Establishment of polarity in angiosperm lateral organs. *Trends Genet.* **18**, 134-141.
- Bowman, J. L., Sakai, H., Jack, T., Weigel, D., Mayer, U. and Meyerowitz, E. M. (1992). *SUPERMAN*, a regulator of floral homeotic genes in *Arabidopsis*. *Development* **114**, 599-615.
- Bowman, J. L., Smyth, D. R. and Meyerowitz, E. M. (1989). Genes directing flower development in *Arabidopsis*. *Plant Cell* **1**, 37-52.
- Bowman, J. L., Smyth, D. R. and Meyerowitz, E. M. (1991). Genetic interactions among floral homeotic genes of *Arabidopsis*. *Development* **112**, 1-20.
- Brand, U., Fletcher, J. C., Hobe, M., Meyerowitz, E. M. and Simon, R. (2000). Dependence of stem cell fate in *Arabidopsis* on a feedback loop regulated by *CLV3* activity. *Science* **289**, 617-619.
- Byrne, M. E., Barley, R., Curtis, M., Arroyo, J. M., Dunham, M., Hudson, A. and Martienssen, R. A. (2000). Asymmetric leaves1 mediates leaf patterning and stem cell function in *Arabidopsis*. *Nature* **408**, 967-971.
- Chen, Q., Atkinson, A., Otsuga, D., Christensen, T., Reynolds, L. and Drews, G. N. (1999). The *Arabidopsis* *FILAMENTOUS FLOWER* gene is required for flower formation. *Development* **126**, 2715-2726.
- Clough, S. J. and Bent, A. F. (1998). Floral dip: a simplified method for *Agrobacterium*-mediated transformation of *Arabidopsis thaliana*. *Plant J.* **16**, 735-743.
- Donnelly, P. M., Bonetta, D., Tsukaya, H., Dengler, R. E. and Dengler, N. G. (1999). Cell cycling and cell enlargement in developing leaves of *Arabidopsis*. *Dev. Biol.* **215**, 407-419.
- Elliott, R. C., Betzner, A. S., Huttner, E., Oakes, M. P., Tucker, W. Q., Gerentes, D., Perez, P. and Smyth, D. R. (1996). *AINTEGUMENTA*, an *APETALA2*-like gene of *Arabidopsis* with pleiotropic roles in ovule development and floral organ growth. *Plant Cell* **8**, 155-168.
- Eshed, Y., Baum, S. F., Perea, J. V. and Bowman, J. L. (2001). Establishment of polarity in lateral organs of plants. *Curr. Biol.* **11**, 1251-1260.
- Fletcher, J. C., Brand, U., Running, M. P., Simon, R. and Meyerowitz, E. M. (1999). Signaling of cell fate decisions by *CLAVATA3* in *Arabidopsis* shoot meristems. *Science* **283**, 1911-1914.
- Gleave, A. P. (1992). A versatile binary vector system with a T-DNA organizational structure conducive to efficient integration of cloned DNA into the plant genome. *Plant Mol. Biol.* **20**, 1203-1207.
- Ha, C. M., Kim, G. T., Kim, B. C., Jun, J. H., Soh, M. S., Ueno, Y., Machida, Y., Tsukaya, H. and Nam, H. G. (2003). The *BLADE-ON-PETIOLE 1* gene controls leaf pattern formation through the modulation of meristematic activity in *Arabidopsis*. *Development* **130**, 161-172.
- Hajdukiewicz, P., Svab, Z. and Maliga, P. (1994). The small, versatile Ppzp family of *Agrobacterium* binary vectors for plant transformation. *Plant Mol. Biol.* **25**, 989-994.
- Hempel, F. D. and Feldman, L. J. (1994). Bi-directional inflorescence development in *Arabidopsis thaliana*: acropetal initiation of flowers and basipetal initiation of paraclades. *Planta* **192**, 276-286.
- Hiratsu, K., Ohta, M., Matsui, K. and Ohme-Takagi, M. (2002). The *SUPERMAN* protein is an active repressor whose carboxy-terminal repression domain is required for the development of normal flowers. *FEBS Lett.* **514**, 351-354.
- Isernia, C., Bucci, E., Leone, M., Zaccaro, L., di Lello, P., Digilio, G., Esposito, S., Saviano, M., di Blasio, B., Pedone, C. et al. (2003). NMR Structure of the single QALGGH zinc finger domain from the *Arabidopsis thaliana* *SUPERMAN* protein. *ChemBiochem.* **4**, 171-180.
- Kerstetter, R. A., Bollman, K., Taylor, R. A., Bomblies, K. and Poethig, R. S. (2001). *KANADI* regulates organ polarity in *Arabidopsis*. *Nature* **411**, 706-709.
- Klucher, K. M., Chow, H., Reiser, L. and Fischer, R. L. (1996). The *AINTEGUMENTA* gene of *Arabidopsis* required for ovule and female gametophyte development is related to the floral homeotic gene *APETALA2*. *Plant Cell* **8**, 137-153.
- Krizek, B. A. (1999). Ectopic expression of *AINTEGUMENTA* in *Arabidopsis* plants results in increased growth of floral organs. *Dev. Genet.* **25**, 224-236.
- Kumaran, M. K., Ye, D., Yang, W. C., Griffith, M. E., Chaudhury, A. M. and Sundaresan, V. (1999). Molecular cloning of *ABNORMAL FLORAL ORGANS*: a gene required for flower development in *Arabidopsis*. *Sex. Plant Repro.* **12**, 118-122.
- Long, J. and Barton, M. K. (2000). Initiation of axillary and floral meristems in *Arabidopsis*. *Dev. Biol.* **218**, 341-353.
- Long, J. A. and Barton, M. K. (1998). The development of apical embryonic pattern in *Arabidopsis*. *Development* **125**, 3027-3035.
- Lynn, K., Fernandez, A., Aida, M., Sedbrook, J., Tasaka, M., Masson, P. and Barton, M. K. (1999). The *PINHEAD/ZWILLE* gene acts pleiotropically in *Arabidopsis* development and has overlapping functions with the *ARGONAUTE1* gene. *Development* **126**, 469-481.
- Mandel, M. A., Gustafson-Brown, C., Savidge, B. and Yanofsky, M. F. (1992). Molecular characterization of the *Arabidopsis* floral homeotic gene *APETALA1*. *Nature* **360**, 273-277.
- McBride, K. E. and Summerfelt, K. R. (1990). Improved binary vectors for *Agrobacterium*-mediated plant transformation. *Plant Mol. Biol.* **14**, 269-276.
- McConnell, J. R. and Barton, M. K. (1998). Leaf polarity and meristem formation in *Arabidopsis*. *Development* **125**, 2935-2942.
- McConnell, J. R., Emery, J., Eshed, Y., Bao, N., Bowman, J. and Barton, M. K. (2001). Role of *PHABULOSA* and *PHAVOLUTA* in determining radial patterning in shoots. *Nature* **411**, 709-713.
- Mizukami, Y. and Fischer, R. L. (2000). Plant organ size control: *AINTEGUMENTA* regulates growth and cell numbers during organogenesis. *Proc. Natl. Acad. Sci. USA* **97**, 942-947.
- Moore, I., Galweiler, L., Grosskopf, D., Schell, J. and Palme, K. (1998). A transcription activation system for regulated gene expression in transgenic plants. *Proc. Natl. Acad. Sci. USA* **95**, 376-381.
- Moussian, B., Schoof, H., Haecker, A., Jurgens, G. and Laux, T. (1998). Role of the *ZWILLE* gene in the regulation of central shoot meristem cell fate during *Arabidopsis* embryogenesis. *EMBO J.* **17**, 1799-1809.
- Nagai, T., Ibata, K., Park, E. S., Kubota, M., Mikoshiba, K. and Miyawaki, A. (2002). A variant of yellow fluorescent protein with fast and efficient maturation for cell-biological applications. *Nat. Biotech.* **20**, 87-90.
- Nath, U., Crawford, B. C., Carpenter, R. and Coen, E. (2003). Genetic control of surface curvature. *Science* **299**, 1404-1407.
- Newman, K. L., Fernandez, A. G. and Barton, M. K. (2002). Regulation of axis determinacy by the *Arabidopsis* *PINHEAD* gene. *Plant Cell* **14**, 3029-3042.
- Ohta, M., Matsui, K., Hiratsu, K., Shinshi, H. and Ohme-Takagi, M. (2001). Repression domains of class II ERF transcriptional repressors share an essential motif for active repression. *Plant Cell* **13**, 1959-1968.
- Ori, N., Eshed, Y., Chuck, G., Bowman, J. L. and Hake, S. (2000). Mechanisms that control *knox* gene expression in the *Arabidopsis* shoot. *Development* **127**, 5523-5532.
- Palatnik, J. F., Allen, E., Wu, X., Schommer, C., Schwab, R., Carrington, J. C. and Weigel, D. (2003). Control of leaf morphogenesis by microRNAs. *Nature* **425**, 257-263.
- Poethig, R. S. and Sussex, I. M. (1985). The cellular parameters of leaf development in tobacco: a clonal analysis. *Planta* **165**, 170-184.
- Riechmann, J. L. (2002). Transcriptional regulation: A genomic overview. In *The Arabidopsis Book* (ed. C. R. Somerville and E. M. Meyerowitz) American Society of Plant Biologists, Rockville, MD, doi/10.1199/tab.0085, <http://www.aspb.org/publications/arabidopsis/>.
- Sakai, H., Medrano, L. J. and Meyerowitz, E. M. (1995). Role of *SUPERMAN* in maintaining *Arabidopsis* floral whorl boundaries. *Nature* **378**, 199-203.
- Sawa, S., Watanabe, K., Goto, K., Liu, Y. G., Shibata, D., Kanaya, E., Morita, E. H. and Okada, K. (1999). *FILAMENTOUS FLOWER*, a meristem and organ identity gene of *Arabidopsis*, encodes a protein with a zinc finger and HMG-related domains. *Genes Dev.* **13**, 1079-1088.

- Semiarti, E., Ueno, Y., Tsukaya, H., Iwakawa, H., Machida, C. and Machida, Y.** (2001). The *ASYMMETRIC LEAVES2* gene of *Arabidopsis thaliana* regulates formation of a symmetric lamina, establishment of venation and repression of meristem-related homeobox genes in leaves. *Development* **128**, 1771-1783.
- Siegfried, K. R., Eshed, Y., Baum, S. F., Otsuga, D., Drews, G. N. and Bowman, J. L.** (1999). Members of the *YABBY* gene family specify abaxial cell fate in *Arabidopsis*. *Development* **126**, 4117-4128.
- Smyth, D. R., Bowman, J. L. and Meyerowitz, E. M.** (1990). Early flower development in *Arabidopsis*. *Plant Cell* **2**, 755-767.
- van der Graaff, E., Dulk-Ras, A. D., Hooykaas, P. J. and Keller, B.** (2000). Activation tagging of the *LEAFY PETIOLE* gene affects leaf petiole development in *Arabidopsis thaliana*. *Development* **127**, 4971-4980.
- van der Graaff, E., Nussbaumer, C. and Keller, B.** (2003). The *Arabidopsis thaliana rlp* mutations revert the ectopic leaf blade formation conferred by activation tagging of the *LEP* gene. *Mol. Genet. Genomics* **270**, 243-252.
- Waites, R. and Hudson, A.** (1995). *Phantastica* – a gene required for dorsoventrality of leaves in *Antirrhinum majus*. *Development* **121**, 2143-2154.
- Waites, R., Selvadurai, H. R., Oliver, I. R. and Hudson, A.** (1998). The *PHANTASTICA* gene encodes a MYB transcription factor involved in growth and dorsoventrality of lateral organs in *Antirrhinum*. *Cell* **93**, 779-789.
- Weigel, D., Alvarez, J., Smyth, D. R., Yanofsky, M. F. and Meyerowitz, E. M.** (1992). *LEAFY* controls floral meristem identity in *Arabidopsis*. *Cell* **69**, 843-859.